DINAME 2017 - Proceedings of the XVII International Symposium on Dynamic Problems of Mechanics
A. T. Fleury, D. A. Rade, P. R. G. Kurka (Editors), ABCM, São Sebastião, SP, Brazil, March 5-10, 2017

Rocket dynamic loading during road transportation in a tractor semi-trailer

Carlos d'Andrade Souto[1], **Matheus Romero**[2], **Edilson Alexandre Camargo** [1], **Domingos Sávio Aguiar** [3]

[1] Institute of Aeronautics and Space, Division of Integration and Tests, Praça Mal. Eduardo Gomes, 50 - Vila das Acácias São José dos Campos - SP -Brazil ZIP CODE: 12228-015, carloscdas@iae.cta.br, edilsoneac@iae.cta.br

[2] University of Taubate, Mechanical Engineering Department, Aeronautical Undergraduate Course, Rua Quatro de Março, 432 - Centro - Taubaté - SP- Brazil – ZIP Code: 12020-270, matheusromeroo@gmail.com

[3] Institute of Aeronautics and Space, Division of Space Systems, Praça Mal. Eduardo Gomes, 50 - Vila das Acácias São José dos Campos - SP - Brazil ZIP Code: 12228-015 , domingosdsa@iae.cta.br

Abstract: Solid propellant rocket engines are submitted to dynamic loads during its transportation from its factories to its launching sites. The loads in transportation phase usually are different from the launching and flight ones, but should also be taken into account in order to prevent damage in the propellant grain. The Institute of Aeronautics and Space (IAE), has developed a small satellite launcher VLS (Veículo Lançador de Satélites). In a typical VLS launching mission, the solid propellant is loaded in the rocket engine cases (manufactured in another site) in an IAE facility in Jacareí, São Paulo. After that the engines are carried by a truck to São José dos Campos airport where are shipped into a military cargo aircraft to São Luís, Maranhão. Finally it is carried by truck again to Alcântara base where the VLS is assembled by connecting properly the S43 engines, the S44 engine, the payload and other launcher components. Since a part of the rocket engines path to its launch site is travelled by road, the dynamic loads which occur in this phase should be evaluated. In this work the vertical dynamics of a tractor-semitrailer with a S43 solid rocket engine as payload was analyzed. A mathematical model of the vehicle was built in a MATLAB routine. The model for the whole vehicle was obtained by considering the tractor and the semi-trailer as rigid bodies connected by the fifth wheel. The vehicle response to a sinusoidal road profile (described by time domain function) and to a road quality profile described by power spectral density function was calculated. The influence of a deviation in a vehicle parameter (tire stiffness) on the dynamic response of the semi-trailer center of mass was estimated.

Keywords: *vehicle dynamics, tractor-semitrailer, rocket transportation loads*

INTRODUCTION

A launcher rocket vehicle used for suborbital or orbital missions is subjected to strong dynamic loads throughout its operational life. During the conceptual phase these loads must be taken into account by the design team in order to design a rocket capable of fulfill its mission completely. An obvious first step is to estimate the dynamic loads by using numerical modeling, semi-empirical methods or by comparing with similar vehicles.

Solid propellant rocket engines suffer dynamic loadings also during transportation from the engine envelope loading facility to the launching site location. Intense accelerations and motions can affect the propellant and propellant-structure junction which may result in failure during engine operation. Once these loads are different from the operational ones it should be estimated and monitored, like done by Camargo (2013).

Performing computer simulations allows one to estimate the engine dynamic response to loads typical of land transport and evaluate if this loads could be harmful to the engine. Then, if necessary, measures to reduce these loads could be taken.

The present work aims to perform dynamic analysis of a terrestrial vehicle (a tractor truck) and the transport carriage of a rocket engine during ground transportation, extending the work of Romero and Souto (2016).

TRACTOR SEMI-TRAILER - ROCKET ENGINE SET ANALYZED

The set tractor semi-trailer-rocket engine analyzed in this work can be seen in Fig.1 and its dimensions are displayed in Fig.2.

Figure 1 – Tractor semi-trailer-rocket engine analyzed

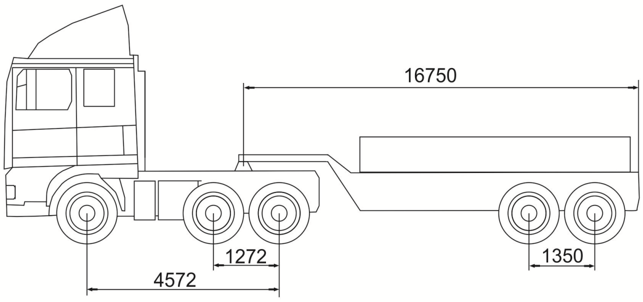

Figure 2 – Tractor semi-trailer dimensions in mm

The dynamic characteristics of the tractor semi-trailer were taken from the characteristics of a similar vehicle analyzed in Plaxico et al (2007). Table 1 displays the vehicle's dynamic properties considered.

Table 1. Tractor semi - trailer characteristics

Mass (Kg)	2631
Moment of Inertia - pitching (Kg.m²)	13709

The tractor suspension data is displayed in Tab.2. Some subsystem data info was not available in Plaxico et al (2007) and so other references were considered. The items marked with * were taken from Deng (2009) and the ones marked with ** in Tabs. 2 and 4 were taken from Elmandany (1987).

Table 2. Tractor suspension properties

Suspension	Stiffness (N/m) (*)	Damping (N.s/m)	Axle mass (Kg)	Tire stiffness (N/m) (*)	Tire damping (N.s/m) (**)
Front	200000	6570	544	980000	700
Intermediate	200000	7790	1043	980000	1200
Rear	200000	7790	1043	980000	1200

The trailer dynamic properties are displayed in Tab.3 and its suspension data is listed in Tab.4.

Table 3. Properties of the set trailer/rocket engine S43/Wooden box.

Set total mass (Kg)	19955
Moment of Inertia – pitching (Kg.m²)	0.27498e+6

Table 4. Suspension properties of trailer

Suspension	Stiffness (N/m) (*)	Damping (N.s/m) (*)	Axle mass (Kg)	Stiffness (N/m) (*)	Tire damping (N.s/m) (**)
Front	1000000	30000	1043	980000	1200
Rear	1000000	30000	1043	980000	1200

MATHEMATICAL MODEL

A mathematical model with two bi - dimensional rigid bodies connected describes the vertical dynamics of the tractor - semi-trailer. The model was obtained by coupling a two and a three axle vehicles. Both vehicles models can be seen in Fig. 3.

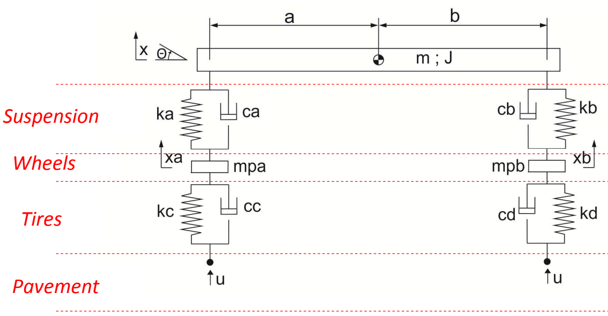

Figure 3- Two axle vehicle

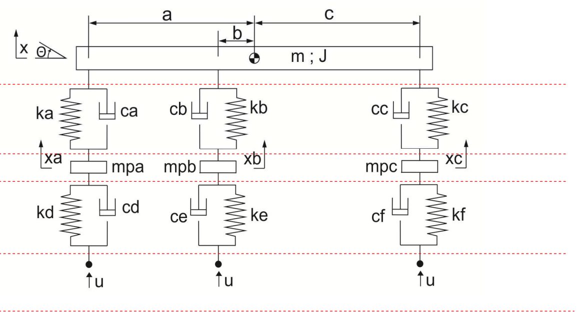

Figure 4- Three axle vehicle

The equations of motion of the two and three axle vehicle were described in Bayrakdar, 2010 and are listed respectively in Eqs. (1-4) and Eqs (5-9) below:

$$m*\ddot{x} = -ka*(x+a*\theta-xa) - kb*(x-b*\theta-xb) - ca*(\dot{x}+a*\dot{\theta}-\dot{xa}) - cb*(\dot{x}-b*\dot{\theta}-\dot{xb}) \quad (1)$$

$$Jy*\ddot{\theta} = -ka*(x+a*\theta-xa)*a + kb*(x-b*\theta-xb)*b - ca*(\dot{x}+a*\dot{\theta}-\dot{xa})*a + cb*(\dot{x}-b*\dot{\theta}-\dot{xb})*b \quad (2)$$

$$mpa*\ddot{xa} = -kc*(xa-u) + ka*(x+a*\theta-xa) - cc*(\dot{xa}-\dot{u}) + ca*(\dot{x}+a*\dot{\theta}-\dot{xa}) \quad (3)$$

$$mpb*\ddot{xb} = -kd*(xb-u) + kb*(x-b*\theta-xb) - cd*(\dot{xb}-\dot{u}) + cb*(\dot{x}-b*\dot{\theta}-\dot{xb}) \quad (4)$$

$$m*\ddot{x} = -ka*(x+a*\theta-xa) - kb*(x-b*\theta-xb) - kc*(x-c*\theta-xc) - ca*(\dot{x}+a*\dot{\theta}-\dot{xa})$$
$$- cb*(\dot{x}-b*\dot{\theta}-\dot{xb}) - cc*(\dot{x}-c*\dot{\theta}-\dot{xc}) \quad (5)$$

$$Jy*\ddot{\theta} = -ka*(x+a*\theta-xa)*a - kb*(x+b*\theta-xb)*b + kc*(x+c*\theta-xc)*c - ca*(\dot{x}+a*\dot{\theta}-\dot{xa})*a$$
$$- cb*(\dot{x}+b*\dot{\theta}-\dot{xb})*b + cc*(\dot{x}+c*\dot{\theta}-\dot{xc})*c \quad (6)$$

$$mpa*\ddot{xa} = -kd*(xa-u) + ka*(x+a*\theta-xa) - cd*(\dot{xa}-\dot{u}) + ca*(\dot{x}+a*\dot{\theta}-\dot{xa}) \quad (7)$$

$$mpb*\ddot{xb} = -ke*(xb-u) + kb*(x-b*\theta-xb) - ce*(\dot{xb}-\dot{u}) + cb*(\dot{x}-b*\dot{\theta}-\dot{xb}) \quad (8)$$

$$mpc*\ddot{xc} = -kf*(xc-u) + kc*(x-c*\theta-xc) - cf*(\dot{xc}-\dot{u}) + cc*(\dot{x}-c*\dot{\theta}-\dot{xc}) \quad (9)$$

For both vehicles equations described in Eqs.(1-9), m is the vehicle mass, Jy is the rotary inertia about the y axis (orthogonal to the paper), a is the distance from the center of mass to the vehicle front, b is the distance from the center of mass to the vehicle rear and u is the displacement imposed by the pavement on the tires.

The dynamic properties (stiffness and damping) of a tire are represented by a coil and a damper in the same way as for each wheel suspension. Each wheel is represented by a mass.

The equations of motion of the vehicles can be written in a matrix form:

$$[M]\{\ddot{x}\} + [C]\{\dot{x}\} + [K]\{x\} = \{F(t)\} \quad (10)$$

For the two axle vehicle the matrices and the coordinate vector are:

$$[M] = \begin{bmatrix} m & 0 & 0 & 0 \\ 0 & Jy & 0 & 0 \\ 0 & 0 & mpa & 0 \\ 0 & 0 & 0 & mpb \end{bmatrix} \quad (11)$$

$$[K]=\begin{bmatrix} (ka+kb) & (ka*a-kb*b) & -ka & -kb \\ (ka*a-kb*b) & (ka*a^2+kb*b^2) & (-ka*a) & (kb*b) \\ -ka & (-ka*a) & (kc+ka) & 0 \\ -kb & (kb*b) & 0 & (kd+kb) \end{bmatrix} \tag{12}$$

$$[C]=\begin{bmatrix} (ca+cb) & (ca*a-cb*b) & -ca & -cb \\ (ca*a-cb*b) & (ca*a^2+cb*b^2) & (-ca*a) & (cb*b) \\ -ca & (-ca*a) & (cc+ca) & 0 \\ -cb & (cb*b) & 0 & (cd+cb) \end{bmatrix} \tag{13}$$

$$\{x\}^T=\{x \quad \theta \quad x\_a \quad x\_b\}^T \tag{14}$$

For the three axle vehicle the matrices and the coordinate vector are:

$$[M]=\begin{bmatrix} m & 0 & 0 & 0 & 0 \\ 0 & Jy & 0 & 0 & 0 \\ 0 & 0 & mpa & 0 & 0 \\ 0 & 0 & 0 & mpb & 0 \\ 0 & 0 & 0 & 0 & mpc \end{bmatrix} \tag{15}$$

$$[K]=\begin{bmatrix} (ka+kb+kc) & (ka*a+kb*b-kc*c) & -ka & -kb & -kc \\ (ka*a+kb*b-kc*c) & (ka*a^2+kb*b^2+kc*c^2) & (-ka*a) & (-kb*b) & (kc*c) \\ -ka & (-ka*a) & (kd+ka) & 0 & 0 \\ -kb & (-kb*b) & 0 & (ke+kb) & 0 \\ -kc & (kc*c) & 0 & 0 & (kf+kc) \end{bmatrix} \tag{16}$$

$$[C]=\begin{bmatrix} (ca+cb+cc) & (ca*a+cb*b-cc*c) & -ca & -cb & -cc \\ (ca*a+cb*b-cc*c) & (ca*a^2+cb*b^2+cc*c^2) & (-ca*a) & (-cb*b) & (cc*c) \\ -ca & (-ca*a) & (cd+ca) & 0 & 0 \\ -cb & (-cb*b) & 0 & (ce+cb) & 0 \\ -cc & (cc*c) & 0 & 0 & (cf+cc) \end{bmatrix} \tag{17}$$

$$\{x\}^T=\{x \quad \theta \quad x\_a \quad x\_b \quad x\_c\}^T \tag{18}$$

The complete vehicle model is shown in Fig.5.

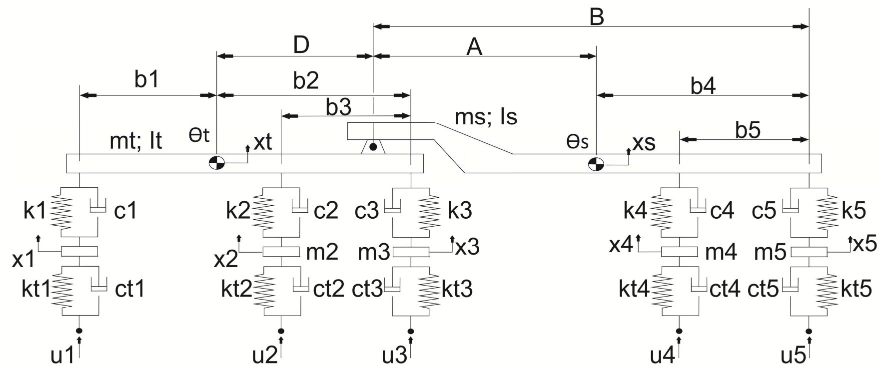

Figure 5- Tractor semi-trailer model

In Fig.5 A, B, D, b1,b2,b3,b4,b5 are dimensions of the complete vehicle. The tractor mass and rotary inertia with respect to axis *y* (orthogonal to the paper) are respectively mt and It; its center of mass vertical and angular displacements are respectively xt and ϴt. In a similar manner, the semi-trailer same properties and coordinates are ms, Is, xs and ϴs. The displacements imposed by the road on the wheels 1 to 5 are u1,u2,...,u5. The tires, wheels and suspension stiffness and damping properties for each wheel are organized as in Figs. 3 and 4.

By coupling the equations of tractor (two axle vehicle) and trailer (three axle vehicle) one can obtain the equations for the complete vehicle:

$$\begin{bmatrix} [M_{tractor}] & \\ & [M_{trailer}] \end{bmatrix} \begin{Bmatrix} \{\ddot{x}_{tractor}\} \\ \{\ddot{x}_{trailer}\} \end{Bmatrix} + \begin{bmatrix} [C_{tractor}] & \\ & [C_{trailer}] \end{bmatrix} \begin{Bmatrix} \{\dot{x}_{tractor}\} \\ \{\dot{x}_{trailer}\} \end{Bmatrix} + \begin{bmatrix} [K_{tractor}] & \\ & [K_{trailer}] \end{bmatrix} \begin{Bmatrix} \{x_{tractor}\} \\ \{x_{trailer}\} \end{Bmatrix} = \begin{Bmatrix} \{F_{tractor}\} \\ \{F_{trailer}\} \end{Bmatrix} \tag{19}$$

Where

$$\{x_{tractor}\} = \{xt \quad \theta t \quad x1 \quad x2 \quad x3\}^T \qquad \{x_{trailer}\} = \{xs \quad \theta s \quad x4 \quad x5\}^T$$

$$\{x^*_{complete\_vehicle}\} = \{xt \quad \theta t \quad x1 \quad x2 \quad x3 \quad xs \quad \theta s \quad x4 \quad x5\}^T$$

The coupling among the vertical motions of the two vehicles in the junction was not included yet in the equations above. This coupling can be deduced from the geometry displayed in Fig.5 (Elmadany, 1988):

$$\frac{xt + D\theta t}{B} = \frac{xs}{(B-A)} \tag{20}$$

Equation (20) can be rewritten as:

$$\theta t = \frac{B}{D(B-A)} xs - \frac{1}{D} xt \tag{21}$$

To consider the coupling, Eq.(21) must be included in the system of equations in Eq.(19). To avoid redundancy of variables, only two of the three variables in Eq.(19) should be included in the full set of equations. The new vector of variables will be:

$$\{x_{complete\_vehicle}\} = \{xt \quad x1 \quad x2 \quad x3 \quad xs \quad \theta s \quad x4 \quad x5\}^T \tag{22}$$

In order to obtain the full set of equations of the complete vehicle a coordinate transformation should be applied to the matrix system in Eq.(19) in this way:

$$[K_{sistema}] = [T]^T [K][T] \qquad [C_{sistema}] = [T]^T [C][T] \qquad [M_{sistema}] = [T]^T [M][T] \tag{23}$$

The transformation matrix [T] can be obtained by considering the transformation from vector $\{x^*_{complete\_vehicle}\}$ to vector $\{x_{complete\_vehicle}\}$:

$$\left\{x^*_{complete\_vehicle}\right\} = [T]\left\{x_{complte\_vehicle}\right\} \tag{24}$$

The matrix [T] is given by:

$$[T] = \begin{bmatrix} 1 & 0 & & & 0 & & & 0 \\ -\alpha/\beta & 0 & & 0 & 1/\beta & 0 & & 0 \\ 0 & 1 & & & 0 & & & \\ & & 1 & & & & & \\ & & & 1 & & & & \\ & & & & 1 & & & \\ & & & & & 1 & & \\ & & & & & & 1 & 0 \\ 0 & & & & & & 0 & 1 \end{bmatrix}_{9x8} \qquad \alpha = 1 - \frac{A}{B} \qquad \beta = D\left(1 - \frac{A}{B}\right) \tag{25}$$

ANALYSES PERFORMED

Calculation of modal parameters

By solving eigenvalue problem given by:

$$([K_{complete\_vehicle}] - \omega^2[M_{complete\_vehicle}])\{X\} = 0 \tag{26}$$

one can obtain natural frequencies and mode shapes for the complete vehicle.

Dynamic response to tire random displacement

The road profile varies randomly and so should be described by using its power spectral density. The forces power spectral densities can then be obtained:

$$S_{fifi}(\omega) = k_i S_{uu}(\omega) \qquad \text{i=1,2,...,6} \tag{27}$$

The off diagonal terms can be neglected and so:

$$([S_{ff}(\omega)] = \begin{bmatrix} 0 & & & & & & & \\ & S_{f1f1}(\omega) & & & & & & \\ & & S_{f2f2}(\omega) & & & & & \\ & & & S_{f3f3}(\omega) & & & & \\ & & & & 0 & & & \\ & & & & & 0 & & \\ & & & & & & S_{f4f4}(\omega) & \\ & & & & & & & S_{f5f5}(\omega) \end{bmatrix} \tag{28}$$

The matrix of power spectral densities of structural responses ($[S_{xx}(\omega)]$) can be calculated by using the relation among the matrix of power spectral densities of applied forces *(*$[S_{ff}(\omega)]$*)* and receptance matrix ($[H(\omega)]$) (Petyt, 1990):

$$[S_{xx}(\omega)] = [\overline{H}(\omega)][S_{ff}(\omega)][H(\omega)]^T \tag{29}$$

The receptance matrix is given by:

$$[H(\omega)] = (-\omega^2[M_{sistema}] + i\omega[C_{sistema}] + [K_{sistema}])^{-1} \quad (30)$$

And its complex conjugate is $[\overline{H}(\omega)]$. The excitation applied by a specific road profile is (Renhberg, 2011):

$$G_d(\omega) = \frac{1}{2\pi v} G_d(n_o)\left(\frac{\omega}{2\pi v n_o}\right)^{-2} \quad (31)$$

Where n_o=0,1m^{-1} , v is the vehicle horizontal speed and $G_d(n_o)$ is a parameter related to the road roughness. In ISO (1995) roads are classified from A (very good) to H (very bad). The better the road quality, the smaller the parameter $G_d(n_o)$. The expression in Eq. 31 can be used as $S_{uu}(\omega)$ in Eq. 27. In this work the value used was $G_d(n_o)$=256x10^{-6} m^3 the same used by Renhberg (2011).

Dynamic response to harmonic displacement applied to the tires

The travelling over a specific road profile defined by a deterministic function can be simulated by applying prescribed displacements to the tires. The force vector in this case will be:

$$\{F\} = \{0 \quad F_1 \quad F_2 \quad F_3 \quad 0 \quad 0 \quad F_4 \quad F_5\}^T \quad (32)$$

By considering that the tires were always in contact with the road, the forces can thus be calculated from the displacement $u_i(t)$ imposed by the road:

$$F_1(t) = k_{T1}(u_1(t) - x_1(t)) + c_{T1}(\dot{u}_1(t) - \dot{x}_1(t)) \quad (33)$$
$$F_2(t) = k_{T2}(u_2(t) - x_2(t)) + c_{T1}(\dot{u}_2(t) - \dot{x}_2(t)) \quad (34)$$
$$F_3(t) = k_{T3}(u_3(t) - x_3(t)) + c_{T3}(\dot{u}_3(t) - \dot{x}_3(t)) \quad (35)$$
$$F_4(t) = k_{T4}(u_4(t) - x_4(t)) + c_{T4}(\dot{u}_4(t) - \dot{x}_4(t)) \quad (36)$$
$$F_5(t) = k_{T5}(u_5(t) - x_5(t)) + c_{T5}(\dot{u}_5(t) - \dot{x}_5(t)) \quad (37)$$

A road with a sinusoidal profile has the form (Bayrakdar,2010):

$$\{u(t)\} = \mathrm{Re}\left(Ye^{j\omega_b t}\right) = Y\cos(\omega_b t) \quad (38)$$

Where the frequency of excitation ω_b is dependant of the vehicle speed (***v***) and the road wave length (***L***):

$$\omega_b = \frac{2\pi v}{L} \quad (39)$$

By inserting Eq.(38) in Eqs. (33-37), one obtains:

$$F_1(t) = Y[k_{t1}\cos(\omega_b t) - c_{t1}\omega_b sen(\omega_b t)] \quad (40)$$
$$F_2(t) = Y[k_{t2}\cos(\omega_b t) - c_{t2}\omega_b sen(\omega_b t)] \quad (41)$$
$$F_3(t) = Y[k_{t3}\cos(\omega_b t) - c_{t3}\omega_b sen(\omega_b t)] \quad (42)$$
$$F_4(t) = Y[k_{t4}\cos(\omega_b t) - c_{t4}\omega_b sen(\omega_b t)] \quad (43)$$
$$F_5(t) = Y[k_{t5}\cos(\omega_b t) - c_{t5}\omega_b sen(\omega_b t)] \quad (44)$$

The nodal displacements can then be calculated by using:

$$\{x\} = \left(-\omega^2[M] + j\omega[C] + [K]\right)^{-1}\{F\} \quad (45)$$

RESULTS

A MATLAB routine was created to calculate the eigenvalues and eigenvectors of the system, its dynamic response in the coordinate *xs* (displacement in the semi-trailer center of mass) when the vehicle travels on roads with a profiles described by Eq.31 and Eq.38.

The matrix system described in Eq.19 was assembled and the modified equation system without the redundant variable was obtained by applying the transformation described in Eqs.(23-25). The matrices thus obtained were used in the calculation of the eigen frequencies and mode shapes by solving the eigenvalue problem (Eq.26) and to obtain the response to the road profile applied on the tires. A speed of 50 Km/h was considered. Three conditions were simulated: tires stiffness of 80, 100 e 120% of its usual values.

Natural frequencies are listed in Tab.5. The first four mode shapes can be seen in Fig.6. In Fig. 7 is displayed the power spectral density of vehicle displacement when travelling in a road with a profile given by Eq.31.

Table 5. Complete vehicle natural frequencies

Mode	Frequencies [Hz]
1	1.10
2	1.43
3	2.14
4	5.36
5	5.44
6	7.00
7	7.04
8	7.43

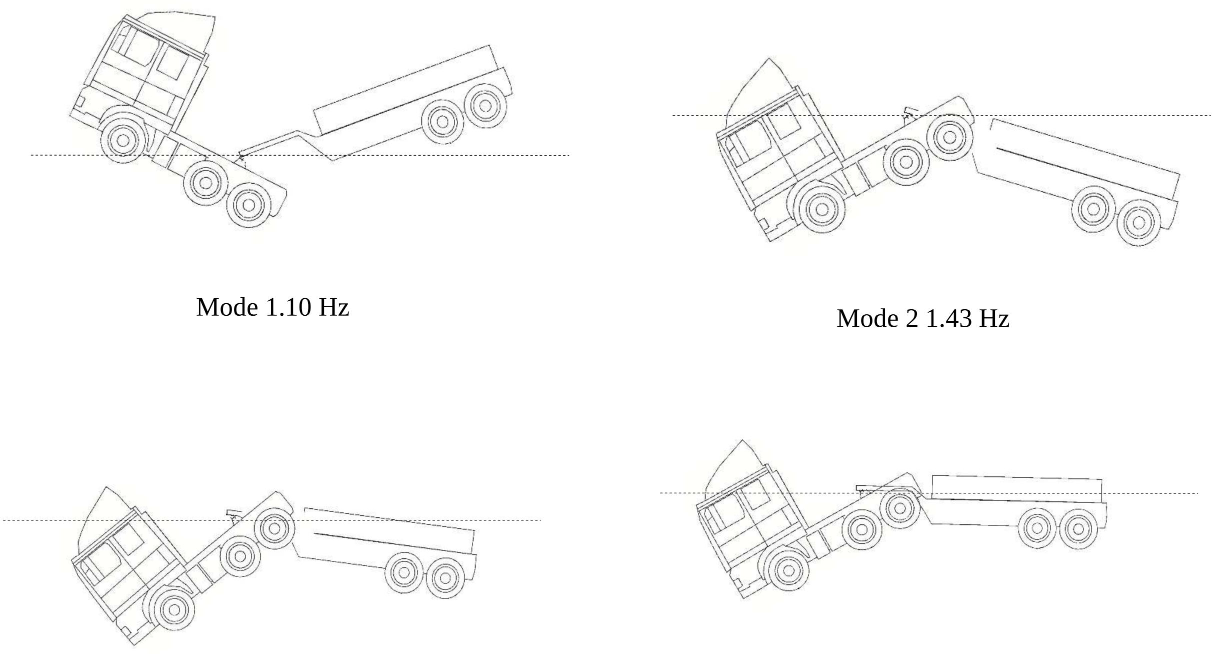

Mode 1.10 Hz

Mode 2 1.43 Hz

Mode 3 2.14 Hz

Mode 4 5.36 Hz

Figure 6 – First four mode shapes for the tractor semi-trailer system

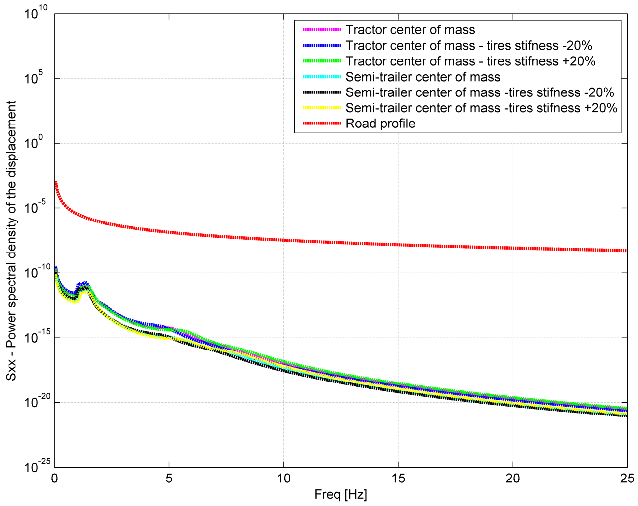

Figure 7 – Power spectral density of the displacement of the complete vehicle center of mass

The response to a sinusoidal road profile (displayed in Fig.8) was also calculated and is show in Fig.9 The same three conditions were also considered.

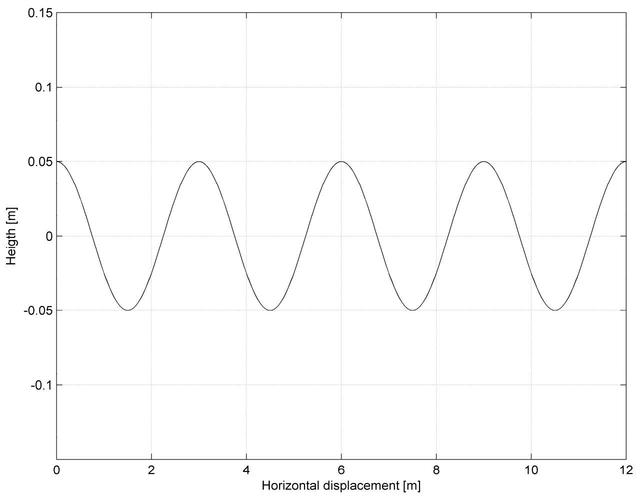

Figure 8 – Road sinusoidal profile

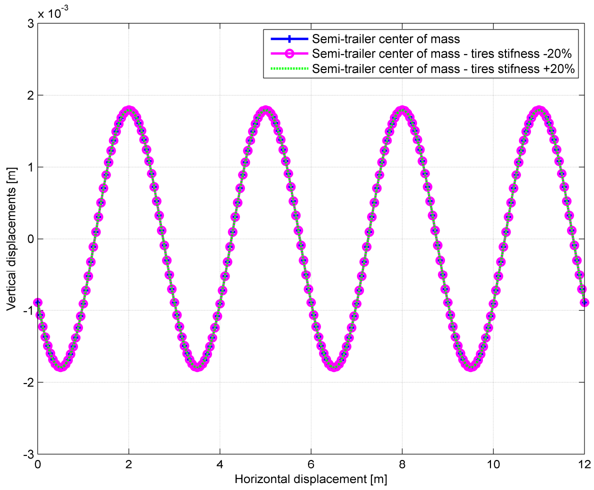

Figure 9 – Response to a road sinusoidal profile in the semi-trailer center of mass

CONCLUSIONS

As should be expected for a heavy vehicle, the natural frequencies are pretty low. By observing Figs. 7,8 and 9, one can conclude that the vehicle suspension absorbs efficiently the road excitations, minimizing the displacement of the semi-trailer center of mass. A deviation of -/+ 20% of the tire stiffness has very little effects in the harmonic and random responses.
In future works, a more detailed sensitivity analysis considering the influence of other vehicle parameters in the dynamic response can be performed. Also, models including flexibility in the vehicle and in the rocket can be considered.

ACKNOWLEDGMENTS

The authors thanks CNPq for the support to this project (undergraduate scholarship for the second author).

REFERENCES

Bayrakdar, Ö. 2010, Random Vibration of a Road Vehicle. 41 p. Master dissertation, İzmir Institute Of Technology, İzmİr, Turkey.
Camargo, E.A.,2013 Measurements of shock and vibration in the transportation of the S43 rocket engine – Salina operation - IAE Internal Report RE 068/AIE/2013
Deng, J., 2009, Adaptation of a trucksim model to experimental heavy truck hard braking data, 177p. Master's dissertation, Ohio State University, EUA
Elmadany, M.M. , 1987, Nonlinear ride analysis if heavy trucks, Computers & Structures Vol. 25 No 1, pp69-82
Elmadany, M.M, 1988, Design and Otimization of Truck Suspension Using Covariance Analysis, Computers & Structures Vol. 28 No 2, pp241-246
International Organization for Standardization (1995), Mechanical vibration – road surface profiles - reporting of data, ISO standard 8608.
Petyt, M.,1990, Introduction to Finite Element Vibration Analysis, Cambridge University Press, Cambridge.
Plaxico, C.; Kennedy, J.; Simonovic, S.; Zisi, N., 2007, Enhanced Finite Element Analysis Crash Model of Tractor-Trailers (Phase A).. 120p Report - National Transportation Research Center Incorporated (NTRCI), University Transportation Center, Knoxville, Tenessee, EUA
Renhberg, A., 2011, Suspension design for off-road construction machines. 92p. PHD thesis – KTH Royal Institute of Technology - Department of Aeronautical and Vehicle Engineering, Stockolm, Sweden.
Romero, M.; Souto C.A., 2016 Dynamic response of a solid rocket engine for land transport, Undergraduate scholarship (CNPq) report, São José dos Campos, Brazil, in Portuguese.

RESPONSIBILITY NOTICE

The authors are the only responsible for the material included in this paper.